

Electrical and optical properties of pure and Pb^{2+} ion doped PVA–PEG polymer composite electrolyte films

V. Krishnakumar · G. Shanmugam

Received: 4 July 2011 / Revised: 4 October 2011 / Accepted: 26 October 2011 / Published online: 16 November 2011
© Springer-Verlag 2011

Abstract Pb^{2+} ion conducting polymer composite electrolyte films, based on polyvinyl alcohol and polyethylene glycol doped with $\text{Pb}(\text{NO}_3)_2$ salt, were prepared using the solution cast technique. X-ray diffraction patterns of polymer composite with salt reveal the decrease in the degree of crystallinity with increasing concentration of the salt. The dielectric plots show an increase in dielectric permittivity at low frequency side with increasing salt concentration as well as temperature. The frequency dependence of ac conductivity obeys the Jonscher power law, and the maximum dc conductivity value is found to be 2.264×10^{-7} S/m at 303 K for the polymer composite with 30 mol% $\text{Pb}(\text{NO}_3)_2$. The activation energy for the ion in polymer electrolyte has been calculated from the modulus plots, and is in good agreement with the activation energy calculated from the temperature-dependent dc conductivity plot. The modulus plots indicate the non-Debye nature of the sample. For pure and doped films at room temperature, the impedance plots exhibit only one semicircle, indicating the presence of one type of conduction mechanism, whereas for 30 mol% salt doped with electrolyte film at different temperatures, it demonstrated the existence of bulk and electrode–electrolyte interface properties. Optical absorption spectra show a broad peak for all complexes, while compared with pure polymer composite, due to the complex formation of polymer electrolyte with $\text{Pb}(\text{NO}_3)_2$ and their absorption edge, direct band gap and indirect band gap were calculated. It was found that the absorption edge and energy gap values decreased on doping with $\text{Pb}(\text{NO}_3)_2$ dopant.

Keywords Polymer composite electrolyte film · Ionic conductivity · Activation energy · Optical absorption spectra and band gap

Introduction

Ion conducting polymers have received considerable attention as electrolyte materials due to their potential applications in electrochemical devices, such as high energy-density batteries, electrochromic devices, chemical sensors [1, 2]. Although these studies revealed many of the properties of these complex systems, the conductivity mechanism is still not fully understood [3]. Usually both crystalline and amorphous phases are present in polymer electrolytes but conductivity mainly occurs in the amorphous phase [4]. The ionic conductivity of polymer electrolytes are strongly affected by various factors such as (1) crystallinity of the material, (2) simultaneous cation and anion motions and (3) the ion-pair formation (anion complex–cation interaction) [5, 6]. These factors reduce the cationic conductivity, and therefore this acts as a barrier for potential applications. To overcome these problems, several approaches were suggested in the literature including the cross-linking of two polymers, addition of fillers and addition of plasticizers in polymer electrolytes. Among these approaches, the plasticization of polymer electrolytes with small organic molecules such as ethylene carbonate (EC), propylene carbonate (PC), dimethyl carbonate (DMC), poly ethylene glycol (PEG) [7, 8] appears to be the simplest approach to improve the ionic conductivity with reduced crystalline phase of polymer electrolytes. These plasticizers help in improving the electrical conductivity of polymer electrolytes by (1) increasing the amorphous content of polymer electrolytes; (2) dissociating ion aggregates present

V. Krishnakumar (✉) · G. Shanmugam
Department of Physics, Periyar University,
Salem 636011, India
e-mail: vkrishna_kumar@yahoo.com

in polymer electrolytes; (3) by lowering the glass transition temperature, T_g .

Among the plasticizers, PEG is a well-known plasticizer [9]. On the other hand, it has been shown that the oxygen atom present on the polyether chain acts as an electron acceptor. The cation of salt forms transient cross-links with the chain segment by coordinating with the oxygen atom on the polymer backbone and thus leads to polymer–salt interaction [10]. However, plasticized polymer electrolytes have several major drawbacks: solvent volatility and poor mechanical properties due to the high degree of plasticization [11–14]. Therefore, the improvement of mechanical properties supporting high ionic conductivity is required for plasticized polymer electrolytes. The incorporation of host polymer significantly changes their physical properties, which is used as phase separator and mechanically rigid network that provides desired mechanical strength to the polymer electrolytes. Compared to other host polymers, polyvinyl alcohol (PVA) has been mainly used as host polymer because it is a water-soluble hydrophilic polymer with a high mechanical strength, good charge storage capacity, dopant-dependent electrical and optical properties [15].

Fenton et al. [16] and Armand et al. [17] have reported that alkali metal salt association complexes with polyethylene oxide (PEO) have significant ionic conductivities. Apart from alkali metal salt-based polymer electrolytes, transition and other metal elements, e.g., Cu [18], Ag [19], Pb [20] and Fe [21], have been studied extensively as dopants in various polymers with the aim of improving its electrical conductivity. Among them, Pb is a particularly important material because of its superconductivity and high reactivity. Although it is toxic, its mean value of toxicity is lower than that of Co [22]. Thus, the addition of Pb reduces the net toxicity of the system. Moreover, Pb is reported to be doped into some superconductor materials to increase the carrier concentration and the enhancement of the electrical conductivity [23]. Because of the homogeneous distribution and good connectivity between the grains in Pb-doped samples, an improvement in electrical

conductivity can be expected. In view of these factors, the present work aims to report the PVA/PEG polymer composite electrolyte films doped with various concentrations of $\text{Pb}(\text{NO}_3)_2$ which have been prepared by solution cast technique. The preparation method used in this work is a very attractive way to produce films. In addition, no complex instrumentation is needed and the synthesis of the films is simple. The effect of the doping of Pb ion on the structural, conductivity and optical properties of these electrolyte films have been studied in detail.

Experimental

Laboratory-grade PVA (MW 14,000; Kemphasol, India), polyethylene glycol (MW 6000, Himedia, India) and lead nitrate (Qualigens, India) were used in this study. Thick films of PVA/PEG and $\text{Pb}(\text{NO}_3)_2$ doped PVA/PEG polymer composite electrolyte films were prepared by the solution cast technique. The polymer composite ratio was fixed as 75:25 wt.% for all films. The lead nitrate salts doped with polymer electrolyte films were prepared by varying the salt concentration (Table 1). An appropriate amount of PVA, PEG and $\text{Pb}(\text{NO}_3)_2$ were dissolved in distilled water and the solutions were stirred for several hours at room temperature to obtain a homogeneous solution. Then, the resulting solutions were cast onto glass Petri dishes and allowed to evaporate the solvent at room temperature until solvent-free films were obtained. X-ray diffraction (XRD) of these films was performed by means of the Rigaku Miniflex-II desktop X-ray diffractometer in the range of $10\text{--}60^\circ$ using $\text{CuK}\alpha$ radiation ($\lambda=1.5406\text{ \AA}$). The dielectric analysis and electrical conductivity study of the polymer electrolyte were carried out in the temperature range of $303\text{--}413\text{ K}$ over a frequency range of $100\text{ Hz--}1\text{ MHz}$ using N4L Phase Sensitive Multimeter interfaced with Impedance Analyzer with a cell with stainless steel electrodes. Optical absorption spectra were recorded at room temperature in the wavelength region $200\text{--}800\text{ nm}$ using the Perkin-Elmer LAMBDA 35 UV–VIS–NIR spectrometer.

Table 1 σ_{dc} , σ_{ac} , σ_0 , A , n , absorption edge and band gap values of PVA/PEG+x mol% $\text{Pb}(\text{NO}_3)_2$, for different $\text{Pb}(\text{NO}_3)_2$ concentration (x) at room temperature

x	$\sigma_{\text{dc}} \times 10^{-7}$ (S/m)	$\sigma_{\text{ac}} \times 10^{-5}$ (S/m)	$\sigma_0 \times 10^{-7}$	$A \times 10^{-10}$	n	Absorption edge	Band gaps (eV)	
							Direct	Indirect
0	0.301	0.360	0.544	0.086	0.93	6.13	6.27	5.99
10	1.303	0.529	0.645	0.174	0.91	5.24	5.38	5.06
20	1.600	0.938	0.852	0.674	0.85	5.10	5.21	5.00
30	2.264	1.992	2.158	5.653	0.75	5.03	5.15	4.96

Results and discussions

XRD studies

Figure 1 shows the XRD patterns of $\text{Pb}(\text{NO}_3)_2$ salt, pure and doped PVA/PEG polymer composite electrolyte films with different concentrations of $\text{Pb}(\text{NO}_3)_2$. In Fig. 1a, the well-defined sharp peaks were observed for $\text{Pb}(\text{NO}_3)_2$ salt, indicating its crystalline nature. These peaks disappear in salt doped polymer electrolyte films. The absence of peaks regarding $\text{Pb}(\text{NO}_3)_2$ salt in the PVA/PEG reveals the complete dissolution of salt in polymer composites. Pure PVA/PEG electrolyte film (Fig. 1b) exhibits two characteristic diffraction peaks of PVA: a minimum intensity peak at 14° and a relatively more intensive peak at 16.7° [24]. No such well-defined sharp peaks attributable to PEG could be observed. It indicates the amorphous nature of PEG. These observations confirm that the present polymer composite electrolyte system possess multiphase, possessing both crystalline and amorphous nature. However, upon the addition of $\text{Pb}(\text{NO}_3)_2$ to the PVA/PEG electrolyte system (Fig. 1c–e), the intensity of these peaks decreases gradually, suggesting a decrease in the degree of crystallinity of the complex. Hodge et al. [25] established a correlation between the intensity of the peak and the degree of the crystallinity. They reported that the intensity of XRD peaks decreases as the amorphous nature increases with the addition of dopant. In the present XRD patterns, no sharp peaks were observed for higher concentrations of $\text{Pb}(\text{NO}_3)_2$ salt in the PVA/PEG, indicating that the amorphous phase was dominant [26]. This amorphous nature results in greater ionic diffusivity with a high ionic conductivity, which can be obtained in amorphous

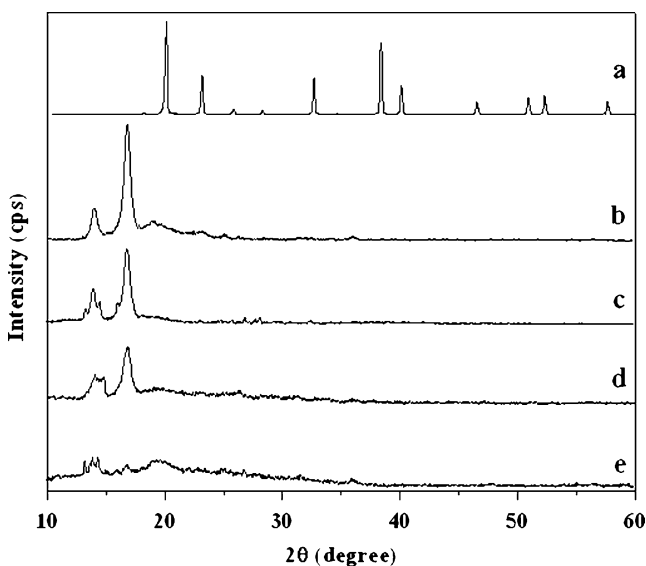


Fig. 1 XRD patterns of **a** $\text{Pb}(\text{NO}_3)_2$ salt, **b** pure PVA/PEG, **c** PVA/PEG with 10 mol% $\text{Pb}(\text{NO}_3)_2$, **d** PVA/PEG with 20 mol% $\text{Pb}(\text{NO}_3)_2$, **e** PVA/PEG with 30 mol% $\text{Pb}(\text{NO}_3)_2$

polymers that have flexible backbone [27, 28]. This is confirmed by conductivity studies.

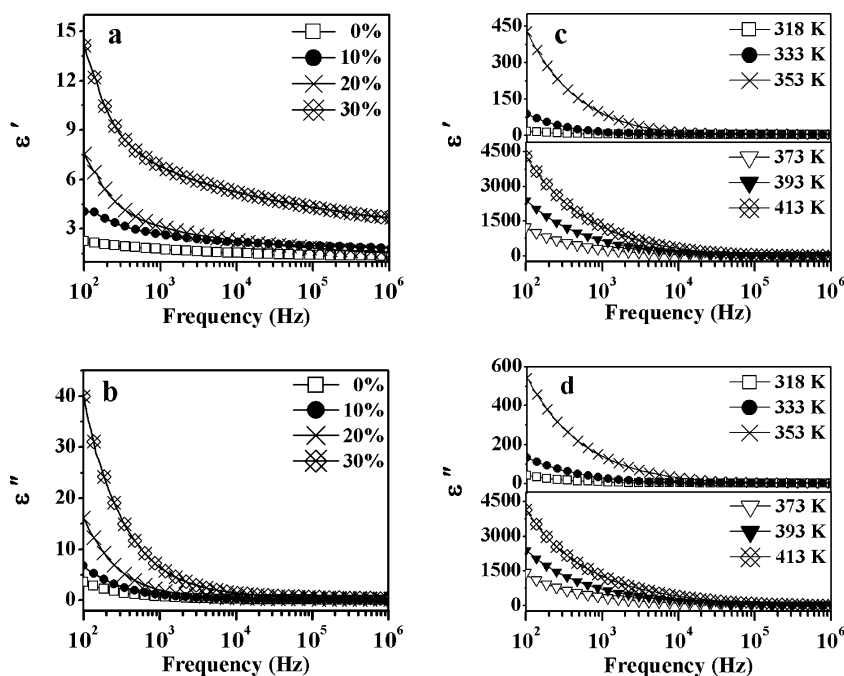
Dielectric properties

Figure 2 shows the frequency dependence of the real (ϵ') and imaginary (ϵ'') parts of the dielectric permittivity of the polymer composite electrolyte films. The room temperature dielectric plots of various concentrations of $\text{Pb}(\text{NO}_3)_2$ doped electrolyte films are shown in Fig. 2a and b. A high value of dielectric permittivity has been observed in the case of $\text{Pb}(\text{NO}_3)_2$ -doped polymer electrolyte films in comparison with the pure PVA/PEG film, and the dielectric permittivity increases with the increase in the salt concentration. It indicates that the introduction of $\text{Pb}(\text{NO}_3)_2$ increases the dielectric permittivity of the PVA/PEG polymer composite electrolyte films. Figure 2c and d shows the dielectric plots of 30 mol% salt doped polymer electrolyte film at different temperatures. It has been observed that the dielectric permittivity increased with increasing temperature. Figure 2 shows that the low frequency dispersions are very strong and can be associated with space charge polarization effects arising from the electrodes. The decrease in dielectric permittivity with increasing frequency can be associated to the inability of dipoles to rotate rapidly leading to a lag between frequency of oscillating dipole and that of applied field. Hence, the dielectric permittivity decreases with increasing frequency [18].

ac conductivity analysis

The frequency dependent ac conductivity of PVA/PEG+x mol% $\text{Pb}(\text{NO}_3)_2$ electrolyte films for (a) different values of x at room temperature and (b) for $x=30\%$ at different temperatures is shown in Fig. 3. It has been observed (Fig. 3a) that as the concentration of lead salt increases, the transition region from the dc plateau to the ac conductivity dispersion region shifts towards the higher frequency range. The conductivity increases with the increase of the number of charge carriers by the addition of $\text{Pb}(\text{NO}_3)_2$. Hence, the mobility of anions is restricted and the enhancement of conductivity is only due to the mobility of Pb cations. It confirms that there is no formation of electrolyte concentration gradients in the films. The ac electrical conductivities of PVA/PEG+ $\text{Pb}(\text{NO}_3)_2$ electrolyte films are higher than those of the pure PVA/PEG film and the conductivity has been found to be high, 1.992×10^{-5} S/m for 30 mol% $\text{Pb}(\text{NO}_3)_2$ doped polymer electrolyte film at room temperature. High values of conductivity obtained for these polymer composite electrolytes might be due to the amorphous nature of the blended polymer matrix and decrease in glass transition temperature. The ac electrical conductivity shows a frequency-independent

Fig. 2 Frequency dependence of **a** real (ϵ') and **b** imaginary (ϵ'') parts of dielectric permittivity for the different concentrations of $\text{Pb}(\text{NO}_3)_2$ electrolyte at room temperature and frequency dependence of **c** real (ϵ') and **d** imaginary (ϵ'') parts of dielectric permittivity of 30 mol % $\text{Pb}(\text{NO}_3)_2$ at different temperatures



plateau in the low frequency region, which corresponds to the dc conductivity of the bulk material, and dispersion at high frequency, which corresponds to the ac conductivity. This behavior obeys the Jonscher power law [29, 30] as given below:

$$\sigma(\omega) = \sigma_0 + A\omega^n \tag{1}$$

where σ_0 is the dc conductivity (frequency-independent plateau in the low frequency region), A is the pre-exponential factor and n is the fractional exponent between 0 and 1. The values of σ_0 , A and n obtained by fitting the Jonscher power law are given in Table 1 (for Fig. 3a). The effect of electrode polarization is evidenced by small deviation from σ_{dc} (plateau region) value in the conductivity plot (in the low frequency region). The n values of these materials are in the range 0.75–0.93 (Table 1). For electrolyte, n values can be between 1 and 0.5, indicating the ideal long-range pathways and diffusion limited hopping (tortuous pathway), respectively [31–33]. With the increase in temperatures, the low frequency electrode polarization phenomena become more prominent, and thus plateau region shifts to the higher frequency side (Fig. 3b). This increase in conductivity with increasing temperature can be related to the increase in the number of mobile charge carriers contributing to the transport of ions.

Complex impedance studies

Figure 4 shows the complex impedance plots of pure and $\text{Pb}(\text{NO}_3)_2$ doped PVA/PEG polymer composite electrolyte films at room temperature. These films exhibited one impedance semicircular arc over wide range of frequency.

The semicircular arcs are representative of the bulk properties of grains (dc resistivity). Thus, the complex impedance relaxation can be explained by using the Cole–Cole-type relaxation. The extrapolation of intercept of the semicircular arc with the real axis (Z') at low frequency (end) gives rise to the bulk resistance (R_b) of the electrolyte system. It is interesting to note that the R_b of pure electrolyte film is higher than the R_b of doped electrolyte films. Thus, the R_b decreases with increase in salt concentration. The ionic conductivity (σ_{dc}) of electrolyte films has been calculated by the following standard relation [34], $\sigma_{dc} = d/R_b A$, where d and A are the thickness and area of the sample. The ionic conductivity values of different

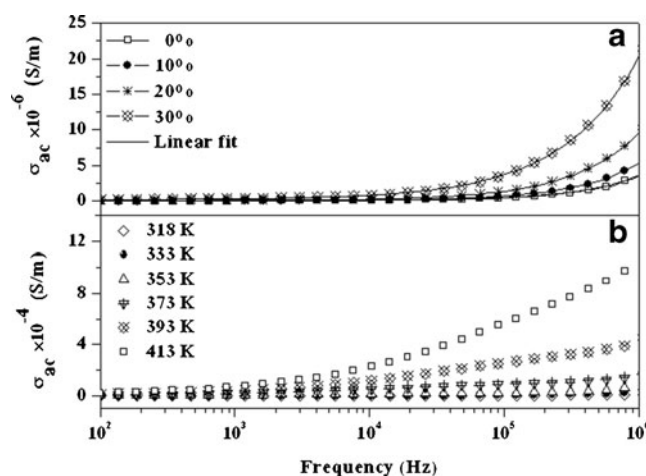


Fig. 3 Frequency dependent ac conductivity of **a** PVA/PEG composite electrolyte films with different concentration of $\text{Pb}(\text{NO}_3)_2$ at room temperature; **b** 30 mol% $\text{Pb}(\text{NO}_3)_2$ -doped PVA/PEG composite electrolyte film at different temperatures

complexes at room temperature are summarized in Table 1. It can be observed from Table 1 that the conductivity of 30 mol% salt doped electrolyte film exhibits the highest conductivity compared with other electrolyte films. The ionic conductivity increased by 1 order of magnitude with the addition of 10 mol% of $\text{Pb}(\text{NO}_3)_2$, which is due to the increased Pb^{2+} charge carriers in the system. The increase in ionic conductivity (inset of Fig. 4) with the addition of salt is attributed to a reduction in crystallinity of polymer electrolyte and the increase in number of mobile charge carriers. This is because the interaction between polymer and $\text{Pb}(\text{NO}_3)_2$ salt leads to high dispersion, so that the conductivity increased.

Figure 5 shows the complex impedance plots of PVA/PEG/30 mol% $\text{Pb}(\text{NO}_3)_2$ electrolyte film at different temperatures. It shows a semicircular arc and inclined spike, which together are the characteristic behavior of ionically conducting solids with blocking electrodes [35]. The semicircle is due to the parallel combination of bulk properties of the electrolyte system. The presence of the depressed semicircle reveals the non-Debye nature of the sample [36] due to the potential well for each site, through which the ion transport takes place, not being equal. The inclined spike represents the formation of the double layer capacitance at the electrode–electrolyte interface due to the migration of ions at low frequency. The electrode double layer at each interface possesses increasing impedance against ion transfer with a decrease in frequency, which, in the Nyquist plot of impedance spectra, was represented by an inclined spike [37]. Furthermore, the inclination of the spike at an angle of less than 90° to the real axis is due to the roughness of the electrode–electrolyte interface [38]. It should be noted that the diameter of the semicircle of high

frequency region decreases with the rise in temperature, and finally it vanishes above 393 K, leaving only a spike in the plot. The disappearance of semicircle at high temperature indicates the conduction is mainly due to the migration of ions. It is evident from the plots that the intercept of the semicircle (R_b) on the real axis tends to lower values with increasing temperature, i.e., σ_{dc} is found to increase with the increase in temperature. The increase in ionic conductivity with temperature, as depicted in Fig. 6, obeys the Arrhenius-type thermally activated process represented by

$$\sigma_{dc} = \sigma_0 \exp\left(\frac{-E_a}{kT}\right) \tag{2}$$

where σ_0 is the pre-exponential factor, E_a is the activation energy, k is the Boltzmann constant and T is the absolute temperature. When the temperature increases, the fraction of free volume and segmental mobility in the electrolyte also increases. They permit the ions to hop from one site to another site, thus increasing the conductivity. This hopping mechanism indicates that more ions gained kinetic energy via thermally activated hopping of ions between trapped sites [19]. The activation energy is found to be 0.127 eV. A low value of E_a is due to the amorphous nature of film that facilitates the fast Pb-ion motion in the polymer chain, and also provides a higher free volume in the electrolyte on increasing temperature [39]. This could lead to greater ionic diffusion which in turn increases the ionic conduction.

Electrical modulus formalism

Figure 7 shows the real (M') and imaginary (M'') parts of electric modulus for polymer composite electrolyte films. Generally, the dielectric materials, having the contribution of electrode polarization effect in their measured dielectric properties, show a plateau at lower frequencies and an abrupt increase in M' spectra at higher frequencies. The room temperature electric modulus spectra of various compositions are shown in Fig. 7a and b. It can be observed that the values of M' (Fig. 7a) for electrolyte films at low frequency are small, which confirms the removal of electrode polarization and it should also be noted that the value of M' decreases with increasing the concentration of $\text{Pb}(\text{NO}_3)_2$. As shown in Fig. 7b, the values of M'' show an asymmetric peak approximately centered in the dispersion region of M' . The peak shifts to higher frequency as the conductivity increases, indicating that the relaxation time decreases as conductivity increases. The conductivity relaxation times can be calculated from the relation [29], $2\pi f_{\max} = 1/\tau_\sigma$, where τ_σ is the conductivity relaxation time and f_{\max} is a frequency corresponding to M''_{\max} . The graph also shows that the height of the peak decreases with the increase in salt concentration as

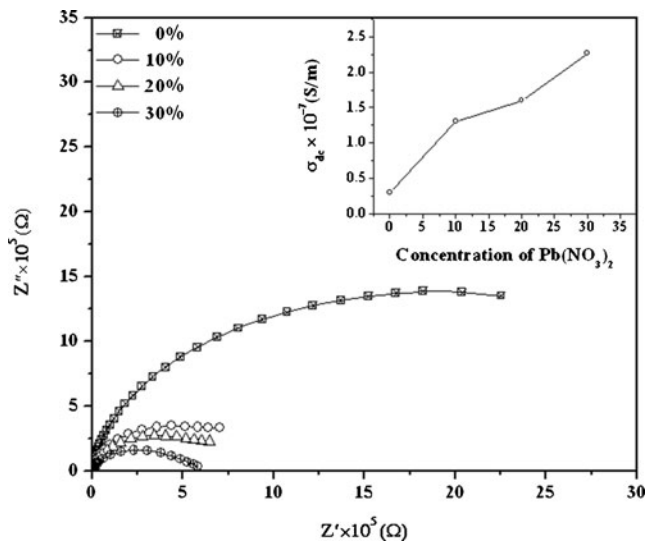
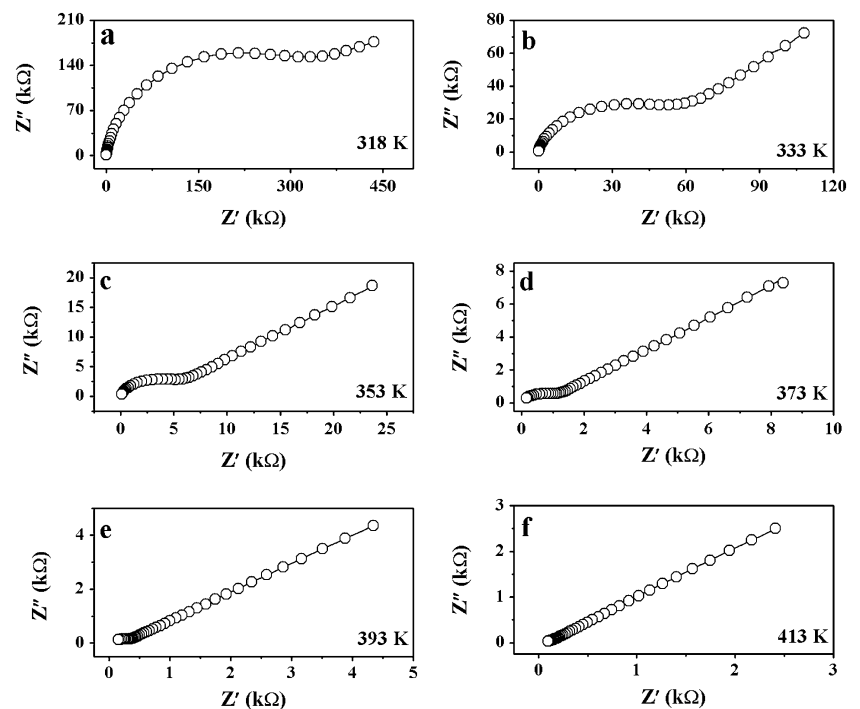


Fig. 4 Complex impedance plots for pure and $\text{Pb}(\text{NO}_3)_2$ -doped PVA/PEG electrolyte films at room temperature. Inset: σ_{dc} vs. salt concentration plot at room temperature

Fig. 5 Complex impedance plots of PVA/PEG/30 mol% $\text{Pb}(\text{NO}_3)_2$ electrolyte film at different temperatures



relaxation time decreases. The variation in τ_{σ} , as a function of $\text{Pb}(\text{NO}_3)_2$ concentration, is shown in Fig. 7c. It can be seen that the conductivity relaxation times decrease with increasing $\text{Pb}(\text{NO}_3)_2$ salt concentration. The steep decrease in conductivity relaxation time can be explained by an increase in charge carriers' concentration, i.e., an increase in conductivity within the sample as a result of an increase in a number of mobile charge carriers.

Figure 7d and e shows the temperature dependence of electric modulus spectra of 30 mol% of $\text{Pb}(\text{NO}_3)_2$ doped electrolyte film. The conductivity behavior in the frequency domain is more conveniently interpreted in terms of

conductivity relaxation time, τ_{σ} , using electrical modulus (M^*) representation. The M^* representation is now widely used to analyze ionic conductivities by associating a conductivity relaxation time with the ionic process [32]. It is obvious (Fig. 6d) that the asymptotic value of M' at high frequency side shows the dispersion tending towards M_{α} due to conductivity relaxation and indicates the presence of a relaxation time. At the low frequency side, M' approaches zero, indicating that the electrode polarization gives a negligible low contribution of M' and can be ignored when the permittivity data are expressed in this form [40]. In Fig. 6e, the low value of M'' at the low frequency side might be due to the large value of capacitance associated with the electrode polarization effect [41], as a result of accumulation of a large amount of charge carriers at the electrode–polymer electrolyte interface. However, a peak is observed that shifts to higher frequency with increasing temperature. The disappearance of M'' peak at higher temperatures is due to the experimental frequency limitation. The frequency associated with each peak is known as the relaxation frequency and gives the value of τ_{σ} for ions. The activation energy (E_a) has been calculated from the Arrhenius relation as follows:

$$\omega_m = \omega_0 \exp\left(\frac{-E_a}{kT}\right) \quad (3)$$

where ω_0 is the pre-exponential factor, k is the Boltzman constant and T is the absolute temperature. The activation energy (Fig. 7f) calculated from the least-square fit to the data points is 0.12 eV. We have also scaled the imaginary part of electric modulus for 30 mol% of $\text{Pb}(\text{NO}_3)_2$ doped

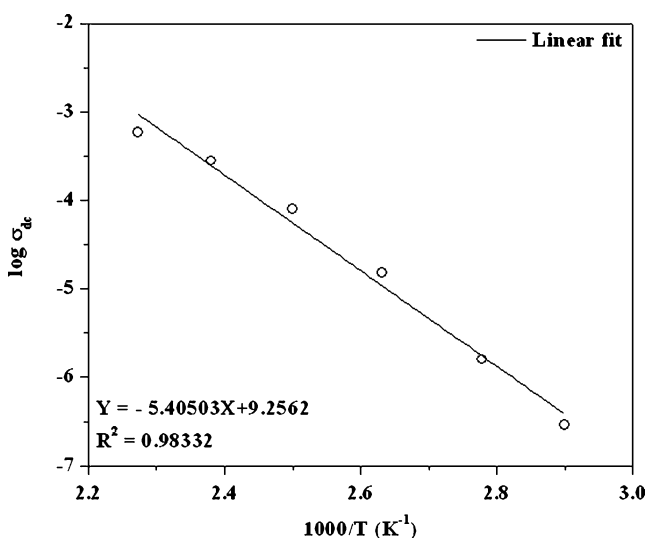
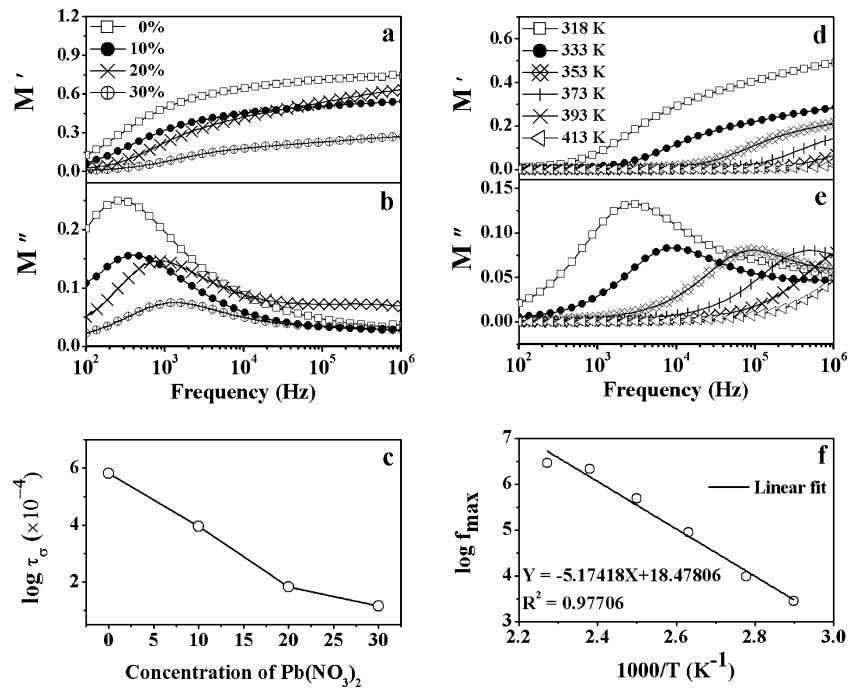


Fig. 6 Inverse temperature dependent dc conductivity of PVA/PEG/30 mol% $\text{Pb}(\text{NO}_3)_2$ electrolyte film

Fig. 7 Frequency dependence of **a** real (M') and **b** imaginary (M'') parts of electric modulus of different mol% of $\text{Pb}(\text{NO}_3)_2$ polymer composite electrolyte films, **c** $\log \tau_\sigma$ vs. concentration of $\text{Pb}(\text{NO}_3)_2$ at room temperature, frequency dependence of **d** real (M') and **e** imaginary (M'') parts of electric modulus of 30 mol% $\text{Pb}(\text{NO}_3)_2$ polymer composite electrolyte films at different temperatures. **f** Inverse temperature dependence of relaxation frequency plot



electrolyte film at different temperatures (Fig. 8). A peak is observed for each M''/M''_{\max} values which shifts towards to higher frequency side due to an increase in temperature. This behavior suggests that the relaxation is activated thermally, and charge carrier hopping is taking place.

Optical properties

Figure 9a shows the absorption spectra of pure and doped polymer composite electrolytes for different concentrations of $\text{Pb}(\text{NO}_3)_2$ at room temperature. It can be seen from the figure that pure polymer composite electrolyte has no absorption peak in the 200 to 400 nm region, while a broad absorption peak in that region was observed for all compositions of $\text{Pb}(\text{NO}_3)_2$ doped polymer electrolyte film. The height of peak increases with increasing concentration of $\text{Pb}(\text{NO}_3)_2$, implying an increasing amount of Pb ions in electrolyte system.

The absorption coefficient (α) was determined from the absorbance (A) using the following relation:

$$I = I_0 \exp(-\alpha x) \tag{4}$$

Hence,

$$\alpha = \frac{2.303}{x} \log\left(\frac{I}{I_0}\right) = \frac{2.303}{xA} \tag{5}$$

where I and I_0 are intensities of incident and transmitted radiations, respectively, x is the thickness of the sample and A corresponds to $\log(I/I_0)$. The optical band gap energy of

the films was estimated from the absorption spectra near the absorption edge. The absorption coefficient dependence on the photon energy is expressed as $(\alpha h\nu) = \beta(h\nu - E_g)^n$, where β is a constant, $h\nu$ is the photon energy, E_g is the optical band gap energy and n is an exponent which can take values of 1, 2, 3, 1/2, and 3/2, depending on the nature of the electronic transitions responsible for the optical band gap. In the present study, the best straight line can be obtained from the values of $n=1/2$ and 2. This suggests that the transition energy for electrons may account for both direct and indirect electron transitions [42]. Davis and Shalliday [43] have also reported that near the fundamental

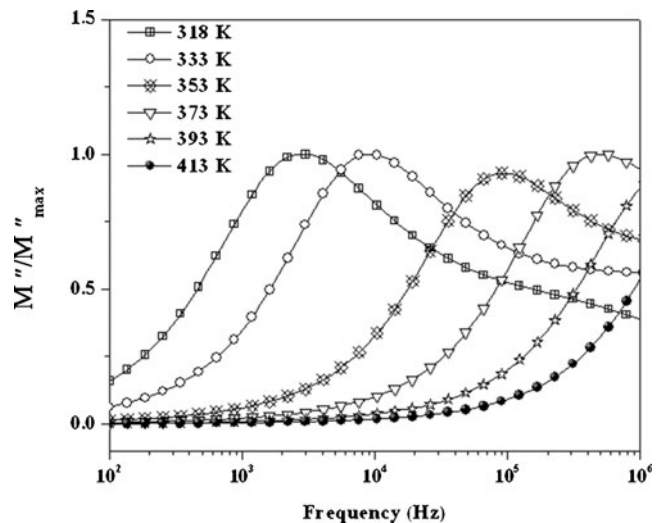
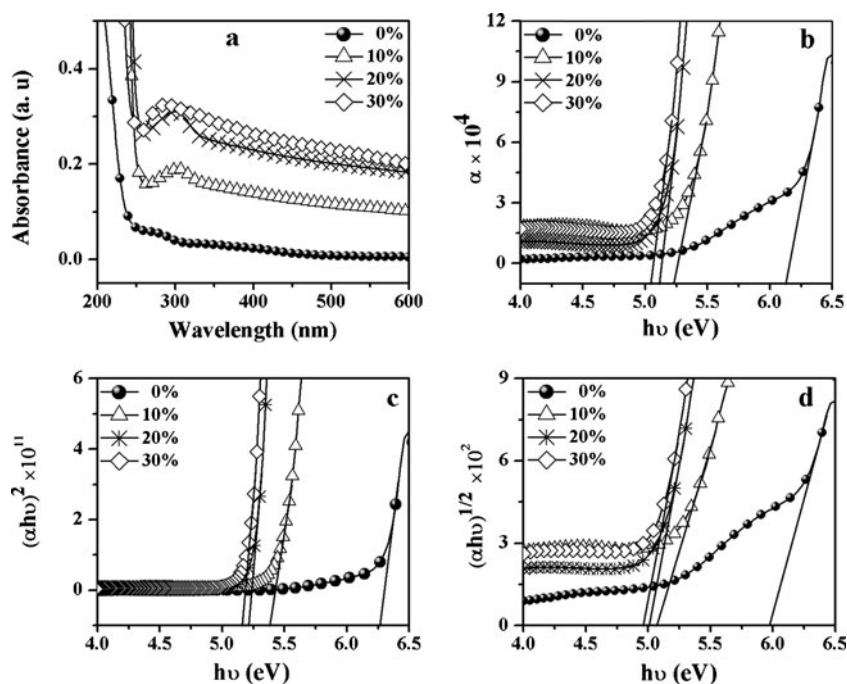


Fig. 8 Scaling behavior of electrolyte film at different temperatures for 30 mol% $\text{Pb}(\text{NO}_3)_2$ electrolyte film

Fig. 9 Pure and $\text{Pb}(\text{NO}_3)_2$ doped PVA–PEG films: **a** absorption spectra, **b** α vs. $h\nu$ plots, **c** $(\alpha h\nu)^2$ vs. $h\nu$ plots, **d** $(\alpha h\nu)^{1/2}$ vs. $h\nu$ plots



band edge, both direct and indirect transitions occur and can be observed by plotting $(\alpha h\nu)^2$ and $(\alpha h\nu)^{1/2}$ as a function of energy $h\nu$. The analysis of Thutupalli and Tomlin [44] is based on the following relations

$$\alpha h\nu = \beta_1 (h\nu - E_{\text{gd}})^{1/2} \quad (6)$$

$$\alpha h\nu = \beta_2 (h\nu - E_{\text{gi}})^2 \quad (7)$$

for direct and indirect electron transitions, respectively, where $h\nu$ is the photon energy, E_{gd} and E_{gi} are the direct band gap and indirect band gap of material, and β_1 and β_2 are the constants. These expressions will be helpful in the determination of the band structure of materials.

The position of the absorption edge was estimated by extrapolating the linear portions of the α vs. $h\nu$ plots (Fig. 9b) to zero absorption value. Figure 9b shows that the absorption edge for pure PVA/PEG electrolyte film lies at 6.13 eV, whereas for 10, 20, 30 mol% $\text{Pb}(\text{NO}_3)_2$ doped polymer composite electrolyte films, the absorption edge values decreased, as shown in Table 1. A plot of $(\alpha h\nu)^2$ vs. $h\nu$ for direct transitions according to Eq. 6 is shown in Fig. 9c. The intercept on the energy axis, on extrapolating the linear portion of the curves to zero absorption value, gives the value of direct band gap. For pure PVA/PEG electrolyte, the direct band gap lies at 6.27 eV, while for 10, 20 and 30 mol% $\text{Pb}(\text{NO}_3)_2$ doped electrolyte films, the values showed a decrease (Table 1). For indirect electron transitions that require phonon assistance, the absorption coefficient depends on the incident photon energy according

to Eq. 7. Hence, the indirect band gap values were obtained from the plots of $(\alpha h\nu)^{1/2}$ vs. $h\nu$ at the intercepts of the energy axis on extrapolating the linear portion of the curves to zero absorption value in Fig. 9d. For pure PVA/PEG polymer composite electrolyte, the indirect band gap lies at 5.99 eV, whereas for 10, 20 and 30 mol% $\text{Pb}(\text{NO}_3)_2$ doped polymer composite electrolyte films, the values are given in Table 1.

In Table 1, it is clear that the band edge, direct band gap and indirect band gap values showed a decrease with the increase in $\text{Pb}(\text{NO}_3)_2$ dopant, which is responsible for the formation of defects in the films. These defects produce the localized states in the optical band gap. These overlaps are responsible for decreasing energy band gap when the concentration of $\text{Pb}(\text{NO}_3)_2$ is increased in the PVA/PEG polymer composite [45]. In other words, the decrease in the optical gap results in an increase in the degree of disorder in the films.

Conclusion

Polymer electrolyte films based on PVA/PEG with lead nitrate as the dopant at different concentrations were prepared using solution cast technique. XRD results confirm the increase in the degree of amorphousity of PVA/PEG with incorporation of salt. The dielectric spectra show that the dielectric permittivity at low frequency increases with increasing $\text{Pb}(\text{NO}_3)_2$ dopant. The ac conductivity spectra obey the Jonscher power law in the high frequency region whereas strong low frequency dispersion

was assigned to the electrode polarization effect. Complex impedance plots indicate that the polymer composite can be effectively doped with $\text{Pb}(\text{NO}_3)_2$ to enhance its conductivity. The increase in conductivity with increasing concentration of dopant is attributed to the formation of charge transfer complexes. It has been observed that the system comprising PVA/PEG electrolyte doped with 30 mol% lead nitrate has the highest conductivity. The activation energy of the dc conductivity is in good agreement with the activation energy of the modulus plots, suggesting that the enthalpy of carrier formation is negligible in the present system. Modulus analysis shows the non-Debye nature for these electrolytes. Optical absorption edge and optical band gaps (both direct and indirect) showed a decreasing trend with increased concentration of the dopant. The results obtained in the present study for PVA/PEG films doped with lead nitrate suggest that the present electrolyte system is a good candidate for electrochemical device applications.

Acknowledgement The authors are thankful to the University Grants Commission (UGC), New Delhi, India, for the financial support of this work.

References

- Fray FM (1991) Solid polymer electrolytes—Fundamentals and technological applications. VCH publishers, New York
- Scrosati B (1993) Applications of electroactive polymers. Chapman and Hall, London
- de Jonge JJ, Van Zon A, de Leeuw SW (2002) Solid State Ionics 147:349–359
- Avellaneda COA, Vieira DF, Al-Kahlout A, Leite ER, Pawlicka A, Aegerter MA (2007) Electrochimica Acta 53:1648–1654
- Pinnavaia TJ, Bell GW (2000) Polymer–clay nanocomposite. Wiley, England
- Aranda P, Ruiz-Hitzky E (1992) Chem Mater 4:1395–1403
- Kumar M, Sekhon SS (2002) Eur Polym J 38:1297–1304
- Tsutsumi H, Matsuo A, Onimura K, Oishi T (1998) Electrochim Solid-State Lett 1:244–245
- MacFarlane DR, Sun J, Meakin P, Fasoulopoulos P, Hey J, Forsyth M (1995) Electrochim Acta 40:2131–2136
- MacCallum JR, Vincent CA (1987) Polymer electrolyte reviews. Elsevier Applied Science, London
- Feuillade G, Perche Ph (1975) J Appl Electrochem 5:63–69
- Watanabe M, Kanba M, Matusuda H, Tsunemi K, Mizoguchi K, Tsuchida E, Shinohara I (1981) Macromol Rapid Commun 2:741–744
- Croce F, Gerace F, Dautzemberg G, Passerini S, Appetecchi GB, Scrosati B (1994) Electrochim Acta 39:2187–2194
- Abraham KM, Alamgir M (1993) J Power Sources 43:195–208
- Abdelkader KA, Anwar Z (2006) J Appl Polym Sci 2:1146–1151
- Fenton BE, Parker JM, Wright PV (1973) Polymer 14:589–592
- Armand M, Chabagno JM, Duclot MJ (1979) In: Vashishta P, Mundy JN, Shenoy GK (eds) Fast ion transport in solids. New York, North-Holland
- Ramya CS, Savitha T, Selvasekarapandian S, Hirankumar G (2005) Ionics 11:436–441
- Hirankumar G, Selvasekarapandian S, Bhuvaneshwari MS, Basakaran R, Vijayakumar M (2006) J Solid State Electrochem 10:193–197
- Bakr NA, Abdel-hamid MI, El-hanafy (1995) J Appl Polym Sci 55:415–420
- Bhattacharya A, De A, Bhattacharya SN, Das S (1994) J Phys Condens Matter 6:10499–10507
- Lukavsky J, Furnadjieva S, Cepak V (2003) Archiv Hydrobiol. Supplementband, Algol Stud 149
- Motohashi T, Nakayama Y, Fujita T, Kitazawa K, Shimoyama J, Kishio K (1999) Phys Rev B 59:14080–14086
- Prajapati GK, Gupta PN (2011) Physica B 406:3108–3113
- Hodge RM, Edwrd GH, Simon EP (1966) Polymer 37:1371–1376
- Mohan VM, Raja V, Sharma AK, Narasimha Rao VVR (2005) Mater Chem Phys 94:177–181
- Mohamad AA, Mohamad NS, Ayahya MZ, Othman R, Ramesh S, Alias Y, Arof AK (2003) Solid State Ionics 156:171–177
- Bhargav PB, Mohan VM, Sharma AK, Narasimha Rao VVR (2007) Int J Polym Mater 56:579–591
- Jonscher AK (1983) Dielectric relaxation in solids. Chelsea Dielectric Press, London
- Jonscher AK (1977) Nature 267:673–679
- Mauritz AK (1989) Macromolecules 22:4483–4488
- Pradhan DK, Choudhary RNP, Samantaray BK (2008) Express Polym Lett 2:630–638
- Sengwa RJ, Choudhary S, Sankhla S (2008) Express Polym Lett 2:800–809
- Majid SR, Arof AK (2007) Physica B 390:209–215
- Prabu M, Selvasekarapandian S, Kulkarni AR, Hiran Kumar G, Sakunthala A (2010) Ionics 16:317–321
- Lanfredi S, Saia PS, Lebullenger R (2002) Solid State Ionics 146:329–339
- Li X, Hsu SL (1984) J Polym Sci Polym Phys Ed 22:1331–1342
- Ramya CS, Selvasekarapandian S, Hiran Kumar G, Savitha T, Angelo PC (2008) J Non-Cryst Solids 354:1494–1502
- Michael MS, Jacob MME, Prabakaran SRS, Radhakrishna S (1997) Solid State Ionics 98:167–174
- Yakuphanoglu F (2007) Physica B 393:139–142
- Patro LN, Hariharan K (2009) Mat Sci Eng B 162:173–178
- Balasubramanyam Achari V, Reddy TJR, Sharma AK, Narasimha Rao VVR (2007) Ionics 13:349–354
- Davis DS, Shalliday TS (1960) Phys Rev 118:1020–1022
- Thutupalli GM, Tomlin G (1976) J Phys D Appl Phys 9:1639–1946
- Abdelaziz M, Ghannam MM (2010) Physica B 405:958–968